C.P. No. 1039

C.P. No. 1039

MINISTRY OF TECHNOLOGY

AERONAUTICAL RESEARCH COUNCIL

CURRENT PAPERS

On the Flexure of a Conical Frustum Shell

by

E. H. *Mansfield, Sc.D.*

LONDON. HER MAJESTY'S STATIONERY OFFICE

1969

PRICE 10s 6d NET

U.D.C. 539.384 : 621-434.1 : 621-434.5 : 621-44.8.1 :
624.078.8 : 621.007 : 629.19.012.25

C.P. No.1039*
October 1967

ON THE FLEXURE OF A CONICAL FRUSTUM SHELL

by

E. H. Mansfield. Sc.D.

SUMMARY

This Report considers theoretically and experimentally some of the problems associated with the flexure of two unequal cylindrical shells Joined by a conical frustum. Particular attention is given to the determination of the overall flexural stiffness of the conical frustum and to structural design considerations associated with the provision of a separation capability in the frustum. The results are particularly relevant to the design of multi-stage rockets.

*Replaces R.A.E. Technical Report 67274 - A.R.C. 30212.

CONTENTS

		Page
1	INTRODUCTION	3
2	SYMBOLS	3
3	ANALYSIS	5
	3.1 The unreinforced conical frustum shell with rigid ends	5
	3.2 The reinforced conical frustum shell with rigid ends	7
	3.3 The effect of non-rigid Junctions at the ends of the frustum	8
	3.4 The conical frustum shell reinforced by four stringers	11
	3.5 The conical frustum shell with a separation capability	17
4	EXPERIMENTS ON XYLONITE CONICAL FRUSTUM SHELLS	21
	4.1 Model dimensions	21
	4.2 The tests	22
	4.3 Test results	23
5	CONCLUSIONS	24
Appendix A	Stresses in an annular plate at the ends of the frustum	25
Appendix B	The loads in the reinforcing rings at the ends of the frustum	27
Appendix C	The loads in the reinforcing rings at separation lines	30
References		32
Illustrations		Figures I-12
Detachable abstract cards		

1 INTRODUCTION

In a multi-stage rocket the structure of each stage is basically a cylindrical shell. When adjacent stages differ in size they may be Joined by a conical frustum shell. At the junctions of the frustum with the cylindrical shells there will be stiffening rings to equilibrate the radial component of the direct stresses in the frustum. The provision of a separation capability in the frustum may also necessitate some internal stiffeners and/or bracing. Indeed, one of the main structural difficulties in providing such a capability lies in the provision of an adequate transverse shear-carrying capacity in the frustum, even when the transverse shears applied are negligible. This is because the direct stresses resisting an applied moment have a transverse component due to the taper.

In this report an analysis is given of the stresses in the frustum due to the remote application of a bending moment. The analysis is kept as simple as possible, consistent with an adequate determination of the overall flexural stiffness of the frustum. This latter information is of particular value in a vibrational analysis, for example, where the rocket may be regarded as a beam of varying rigidity. Attention is also given to structural design considerations associated with the provision of a separation capability. A simplified analysis is presented for optimising the structure to achieve maximum overall flexural stiffness. In addition, a series of model conical frustum shells have been tested to exemplify the relative merits of different types of sheer connection across a separation line.

2 SYMBOLS

A_1, A_2	section areas of reinforcing rings
A'	section areas of reinforcing rings resisting shear, i.e. approximate web area
A_s	section area of stringer
D	$Et^3/12(1-\nu^2)$
E	Young's modulus
F_n	functions of a, β, μ
h	depth of reinforcing ring
EI	flexural stiffness of equivalent beam of length ℓ
EI_1	flexural stiffness of cylinder with properties as at small end of frustum

EI_r	flexural stiffness of reinforcing ring
G	shear modulus
ℓ	axial length of frustum
M	bending moment applied to cylinders remote from frustum
m	bending moment in reinforcing ring
$N_s, N_\theta, N_{s\theta}$	forces per unit length in the shell, see Fig.1
P_1, P_2	hoop loads in reinforcing rings
P_s	direct load in stringer
r	radius of frustum, see Fig.1
s	distance along generators of frustum from cone ape*
t	thickness of shell
t_r	thickness of reinforcing ring
t_s	thickness of stringer-sheet
T_r, T_θ	radial and shear loads per unit length acting on reinforcing ring
U	strain energy in frustum
U_r	strain energy in reinforcing rings
V	shear in reinforcing ring
w	width of reinforcing ring
a	semi-angle of frustum
β	r_2/r_1
Y	introduced before equation (19)
η	I/I_1, non-dimensional flexural stiffness of frustum
θ	angular distance, see Fig.1
μ	$t_{s,1}/t$
ν	Poisson's ratio
σ^*	maximum stress in smaller cylinder due to bending
ψ_1, ψ_2	parameters introduced in equation (16)

Suffices 1, 2 (except after F) refer to small and large end of frustum.

3 ANALYSIS

The following analysis is based on the membrane theory of shells. The simplest problems are treated first and attention is concentrated on the determination of the overall flexural stiffness of the conical frustum.

3.1 The unreinforced conical frustum shell with rigid ends

According to Ref.1 (p.67) the forces per unit length in the shell are given by

$$\left.\begin{aligned} N_s &= \frac{M}{\pi \cos a \sin^2 a}\left(\frac{\cos \theta}{s^2}\right) , \\ N_\theta &= 0 , \\ N_{s\theta} &= \frac{M}{\pi \cos a \sin a}\left(\frac{\sin \theta}{s^2}\right) , \end{aligned}\right\} \qquad (1)$$

where M is the applied moment, a is the semi-angle of the cone and the notation for the forces is as shown in Fig.1.

The strain energy per unit area of the shell is accordingly given by

$$U' = \frac{1}{2Et}\{N_s^2 + 2(1+\nu)\, N_{s\theta}^2\} , \qquad (2)$$

where E is Young's modulus, ν is Poisson's ratio and t is the thickness of the shell. The total strain energy in the shell is thus given by

$$U = \frac{1}{2Et}\int_0^{2\pi}\int_{s_1}^{s_2} \{N_s^2 + 2(1+\nu)\, N_{s\theta}^2\}\, s \sin a \, d\theta \, ds$$

$$= \frac{M^2 \ell (r_1 + r_2)}{4\pi E t\, r_1^2\, r_2^2}\left(\frac{1 + 2(1+\nu)\sin^2 a}{\cos^3 a}\right) , \qquad (3)$$

in virtue of equation (I), where ℓ is the axial length of the frustum and r_1, r_2 are its end. radii ($r_1 < r_2$, say).

Now the strain energy stored in a uniform beam whose flexural stiffness is EI is given by

$$u = \frac{M^2 \ell}{2EI} , \tag{4}$$

so that by equating equations (3) and (4) we can determine the stiffness of an equivalent uniform beam of length ℓ. Furthermore, this stiffness is given conveniently in nondimensional terms by expressing it as a multiple of the stiffness of a cylinder whose skin thickness is t and radius r_1, say. In other words we write

$$\left.\begin{aligned} I &= \eta I_1 , \quad \text{say,} \\ \text{where} \qquad I_1 &= \pi t r_1^3 . \end{aligned}\right\} \tag{5}$$

Thus we find

$$\left.\begin{aligned} \eta &= F_1(\alpha)\ F_2(\beta) \\ \text{where} \qquad F_1(\alpha) &= \frac{\cos^3\alpha}{1 + 2(1+\nu)\sin^2\alpha} , \\ F_2(\beta) &= \frac{2\beta^2}{1+\beta} \\ \text{and} \qquad \beta &= r_2/r_1 . \end{aligned}\right| \tag{6}$$

The parameter η is plotted against β for various values of α in Fig.2. [It is to be noted that as $\alpha \to 0$, $F_1 \to 1$ so that $F_2 I_1$ may be identified as the 'average' overall stiffness of the frustum regarded as a beam of varying stiffness. Thus, had we chosen $F_2 I_1$ instead of I, as our reference stiffness the effect of the angle of taper would have been given simply by the term $F_1(\alpha)$. This, in turn, is given by η as $\beta \to 1$.]

The values of η determined here relate to a frustum with rigid ends; a finite rigidity of the ends results in a further drop in overall stiffness. See section 3.3.

3.2 The reinforced conical frustum shell with rigid ends

Here we consider a shell of constant thickness reinforced by closely spaced stringers lying along the generators of the frustum. The stringers are assumed to be continuous and untapered so that, unlike the skin, their total section ares does not vary axially. The stringers are assumed to be sufficiently close for the concept of a stringer-sheet to be valid.

The forces per unit length in the reinforced shell are again given by equation (1) because they are determined entirely from equilibrium conditions. The strain energy per unit area of the reinforced shell is, however, given by

$$U' = \frac{1}{2E}\left(\frac{N_s^2}{t + t_s} + \frac{2(1+\nu)\, N_{s\theta}^2}{t}\right) , \tag{7}$$

where t_s is the thickness of the equivalent stringer-sheet. Further, if $t_s = t_{s,1}$ at the smeller end of the frustum, we can write

$$t_s = \mu t s_1/s ,$$

where

$$\mu = t_{s,1}/t . \tag{8}$$

Substitution of equations (1) and (8) into (7) and integration yields

$$U = \frac{M^2 \ell (r_1 + r_2)}{4\pi E t\, r_1^2\, r_2^2}\left(\frac{F_3(\beta,\mu)}{\cos^3 a} + \frac{2(1+\nu)\sin^2}{4}\right) ,$$

where (9)

$$F_3(\beta,\mu) = \frac{2\beta}{\mu^2(\beta^2-1)}\left\{\mu(\beta-1) + \beta \ln\left(\frac{\beta+\mu}{\beta(1+\mu)}\right)\right\} ,$$

which is plotted against β for various values of μ in Fig.3.

By equating equation8 (4) and (9) we may determine the stiffness of an equivalent uniform beam. Expressing this as a multiple of the stiffness of a cylinder specified by t, t_s, and r_1 gives, in a manner analogous to equation (5),

$$I = \eta I_1 \ ,$$

where

$$I_1 = \pi t(1+\mu)\ r_1^3 \ , \qquad (10)$$

and

$$\eta = \frac{F_2(\beta)\cos^3\alpha}{(1+\mu)\{F_3(\beta,\mu) + 2(1+\nu)\sin^2\alpha\}} \ .$$

For the particular case in which $\mu = 1$, the parameter η is plotted against β for various values of a in Fig.4.

3.3 The effect of non-rigid junctions at the ends of the frustum

So far the analysis has assumed that the junctions between the conical frustum and the cylinders are rigid. In practice, of course, this is not so and flexibility of these junctions further reduces the overall flexural stiffness of the conical frustum. In this section we assume that these Junctions are reinforced by rings of radius r_1, r_2 and section areas A_1, A_2 respectively. [It transpires that, for this particular loading condition the flexural rigidity of the rings is not an important parameter except in so far as it affects the stability of the rings.] In Appendix A a stress function solution is presented for the case of a deep ring in the form of an annulus of constant thickness.

At a Junction there is equilibrium of the axial components of the forces per unit length in the cylinder and frustum, and the forces acting on the ring are purely radial and shear loads. If these are denoted by T_r and T_θ respectively, we have for the ring at $s = s_1$,

$$T_r = N_s \sin a = \left(\frac{M}{\pi \cos a \sin a}\right)\frac{\cos\theta}{s_1^2} \ ,$$

and (11)

$$T_\theta = N_{s\theta} = \left(\frac{M}{\pi \cos a \sin a}\right)\frac{\sin\theta}{s_1^2} \ .$$

It may be verified that these distributed forces do not cause any bending of the ring but produce a varying hoop load P_1 given by

$$P_1 = \left(\frac{M \tan \alpha}{\pi r_1}\right) \cos \theta \quad . \tag{12}$$

By the same token the hoop load P_2 is given by

$$P_2 = -\left(\frac{M \tan \alpha}{\pi r_2}\right) \cos \theta \quad . \tag{13}$$

The total strain energy stored in the rings is thus given by

$$U_r = \frac{1}{2E} \int_0^{2\pi} \left(\frac{r_1 P_1^2}{A_1} + \frac{r_2 P_2^2}{A_2}\right) d\theta$$

$$= \frac{M^2 \tan^2 \alpha}{2\pi E} \left(\frac{1}{A_1 r_1} + \frac{1}{A_2 r_2}\right) . \tag{14}$$

[We note here that in determining A_1, A_2 allowance may be made for the adjacent shell. skin - an 'edge effect' not accounted for by membrane theory. The effective section areas of skin $(\delta A_1, \delta A_2)$ are approximately the same as those in a continuous cylindrical shell under a ring of radial loads (see Ref.1, p.283) for which

$$\left.\begin{aligned} \delta A_1 &\approx 1.5 \; r_1^{\frac{1}{2}} \; t^{3/2} \; , \\ \delta A_2 &\approx 1.5 \; r_2^{\frac{1}{2}} \; t^{3/2} \; , \end{aligned}\right\} \tag{15}$$

where it is assumed that the thickness of the cylindrical shells adjoining the frustum is the same as that in the frustum.]

The total strain energy in the frustum is the sum of expressions (9) and (14). By equating this sum to expression (4) we can find, as before, the stiffness of an equivalent beam. Representation in non-dimensional form is facilitated by the introduction of the symbols

$$\left.\begin{aligned} \psi_1 &= A_1/r_1 t \ , \\ \psi_2 &= A_2/r_2 t \ , \end{aligned}\right| \qquad (16)$$

whence, corresponding to equation (10), we have

$$\eta = \frac{\cos^3\alpha}{1+\mu}\left[\frac{F_3(\beta,\mu) + 2(1+\nu)\sin^2\alpha}{F_2(\beta)} + \frac{\sin^3\alpha}{\beta - 1}\left(\frac{1}{\psi_1} + \frac{1}{\beta^2\psi_2}\right)\right]^{-1} . \qquad (17)$$

In practice the section areas A_1, A_2 may well be determined by loading conditions other than that of pure bending of the conical frustum. Nevertheless, we determine them below on that basis, but introduce an arbitrary proportionality constant in an attempt to account for other design considerations. Now the maximum direct stress in the frustum is given by

$$\left.\begin{aligned} \frac{N_{s,max}}{t(1+\mu)} &= \sigma^* \ , \quad \text{say} \\ &= \frac{M}{\pi t(1+\mu)\, s_1^2 \cos\alpha \sin^2\alpha} \ , \end{aligned}\right\} \qquad (18)$$

in virtue of equation (1). If we stipulate that the maximum hoop stress in the rings is $\gamma\sigma^*$, say, the areas A_1, A_2 are determined from equations (12) and (13):

$$\left.\begin{aligned} A_1 &= \frac{M\tan\alpha}{\pi r_1 \gamma\sigma^*} = \frac{r_1 t(1+\mu)\sin\alpha}{\gamma} \ , \\ A_2 &= A_1/\beta \ . \end{aligned}\right\} \qquad (19)$$

Substitution of equation (19) into equations (16) and (17) gives

$$\eta = \cos^3\alpha\left[\frac{(1+\mu)\,\{F(\beta,\mu) + 2(1+\nu)\sin^2\alpha\}}{F_2(\beta)} + \frac{2\gamma\sin^2\alpha}{\beta - 1}\right]^{-1} . \qquad (20)$$

For the particular case in which $\mu = 1$, $\gamma = 1$, the parameter η is plotted against β for various values of α in Fig.5.

3.4 The conical frustum shell reinforced by four stringers

Here we assume that the conical frustum shell is reinforced by four equally-spaced stringers - an extreme case in which, of course, the stringer-sheet concept is not appropriate. Because of the inherent limitations of the membrane theory of shells we restrict attention first to the more tractable case in which the stringer section areas increase linearly with the distance s. It is also assumed that there is stringer continuity in the adjoining cylinders. The forces acting on the reinforcing rings at the junctions between the conical frustum and the cylinders now produce bending in the plane of the junctions, and it is necessary to take into consideration the flexural rigidity of the rings. Finally we note that it is only necessary to consider one orientation of the stringers relative to the applied moment because solutions for different orientations may be obtained from it by arguments of symmetry and moment resolution.

Tapered stringers at $\theta = 0, \pm\frac{1}{2}\pi, \pi$

The solution is facilitated by regarding the applied moment M as composed of two parts M' and M", say, in which M' acts on the 'unreinforced' shell producing stresses of the form shown in equation (I), while M" causes direct stresses only in the stringers together with shear in the skin. The relative magnitudes of M' and M" are determined by equality of direct stress (and hence strain) in the stringers and adjacent skin.

Thus we have

$$\left.\begin{aligned} N'_s &= \frac{M'}{\pi \cos a \sin^2 a}\left(\frac{\cos\theta}{s^2}\right) , \\ N'_{s\theta} &= \frac{M'}{\pi \cos a \sin a}\left(\frac{\sin\theta}{s^2}\right) . \end{aligned}\right\} \qquad (21)$$

Also, if P_s is the load in the stringer at $\theta = 0$,

$$M'' = 2P_s s \cos a \sin a , \qquad (22)$$

and equilibrium between the stringer and the adjacent sheets gives

$$\frac{dP_s}{ds} \pm 2N_{s\theta} = 0 ,$$

whence from equation (22), assuming that M" is constant,

$$
\left.\begin{aligned}
N''_{s\theta} &= \frac{M''}{4\cos\alpha\sin\alpha}\,\frac{1}{s^2}\ , \qquad 0 < \theta < \pi\ ,\\
&= -\frac{M''}{4\cos\alpha\sin\alpha}\left(\frac{1}{s^2}\right)\ , \qquad -\pi < \theta < 0\ .
\end{aligned}\right\} \qquad (23)
$$

[It is to be noted that these variations of $N_{s\theta}$ do not require the presence of additional N_s and N_θ terms for equilibrium; the $1/s^2$ variation is the same as that due to a pure torque.]

Now the section area of each stringer A_s is given by

$$
A_s = A_{s,1}\,(s/s_1)\ , \quad \text{say,} \qquad (24)
$$

so that the direct stress in the stringer at $\theta = 0$, is given by

$$
\frac{P_s}{A_s} = \frac{M''s}{2\cos\alpha\sin\alpha .\ A_{s,1}}\left(\frac{1}{s^2}\right)
$$

from equation (22). By equating this to the direct stress associated with $(N'_s)_{\theta=0}$ we obtain

$$
\left.\begin{aligned}
M'' &= \frac{2M'\,A_{s,1}}{\pi r_1 t}\\
&= \mu M'\ , \quad \text{say,}
\end{aligned}\right\} \qquad (25)
$$

following the notation of section 3.2. The total strain energy stored in the shell and stringers is therefore given by

$$
U = \frac{1}{2Et}\int_0^{2\pi}\int_{s_1}^{s_2}\{(N'_s)^2 + 2(1+\nu)(N'_{s\theta} + N''_{s\theta})^2\}\ s\sin\alpha\ d\theta\ ds + \frac{1}{2E}\int_{s_1}^{s_2}\frac{2P_s^2}{A_s}\,ds
$$

$$
= \frac{M^2\ell(r_1 + r_2)}{4\pi Et\ r_1^2\ r_2^2\cos^3\alpha}\left[\frac{1}{1+\mu} + 2(1+\nu)\left\{1 + 0.234\left(\frac{\mu}{1+\mu}\right)^2\right\}\sin^2\alpha\right]\ . \qquad (26)
$$

[It is to be noted that if the stringers had been regarded as a (tapered) stringer-sheet the energy stored would have been the same as that in equation (26) but without the term containing the factor 0.234..]

Stringers of constant section area

An approximate solution may be obtained for the case of untapered stringers by the adoption of equations (21), (22) and (23) with the ratio M''/M' no longer constant but given by

$$\frac{M''}{M'} \approx \frac{2A_s}{\pi r t} = \frac{\mu s_1}{s} \quad . \tag{27}$$

The total strain energy stored in the shell and stringers is now given by

$$U \approx \frac{M^2 \ell (r_1 + r_2)}{4\pi E\, t\, r_1^2 r_2^2 \cos^3 \alpha} \left[F_3(\beta,\mu) + 2(1+\nu)\{1 + F_4(\beta,\mu)\} \sin^2\alpha\right] ,$$

where

$$F_4(\beta,\mu) = 0.234 \left[\frac{\mu^2(\beta-1)^2 + \mu(\beta+1)(\mu^2-3\beta) - 6\beta^2}{\mu(\mu+1)(\mu+\beta)(\beta+1)} + \frac{6\beta^2}{\mu^2(\beta^2-1)} \ln\left(\frac{\beta(1+\mu)}{\beta+\mu}\right)\right] , \tag{28}$$

which is plotted against β for various values of μ in Fig.6.

The loads in the reinforcing rings at the ends of the frustum

The radial and shear loads acting on the reinforcing rings are conveniently expressed in terms of the previous dashed and double-dashed systems. Thus (c.f. equation (II)),

$$T_r = N'_s \sin\alpha + \text{forces } P_s \sin\alpha \text{ at } 0,\pi,$$

and

$$T_\theta = N'_{s\theta} + N''_{s\theta}$$

The dashed components do not cause any bending of the ring but produce a varying hoop load which, in the ring of radius r_1 say, is given by

$$P'_1 = \left(\frac{M' \tan\alpha}{\pi r_1}\right) \cos\theta \quad . \tag{29}$$

It is shown in Appendix B that the double-dashed components produce a varying hoop load of the same form:

$$P_1'' = \left(\frac{M'' \tan \alpha}{\pi r_1}\right) \cos \theta \quad . \tag{30}$$

There are also shearing forces V_1 given by

$$V_1 = \left(\frac{M'' \tan \alpha}{\pi r_1}\right)\left(\frac{\pi}{4} - \sin \theta\right) \quad , \quad 0 < \theta < \pi \quad , \tag{31}$$

and bending moments m_1 given by

$$m_1 = M'' \tan \alpha \left(\frac{\pi}{8} - \frac{\theta}{4} - \frac{1}{\pi} \cos \theta\right) \quad , \quad 0 < \theta < \pi \quad . \tag{32}$$

The total strain energy stored in the ring is likely to be primarily that due to bending with lesser contributions from the hoop loads and sheer forces. Thus

$$U_{r,1} = \frac{1}{2EI_{r,1}} \int_0^{\pi} 2m_1^2 \, r_1 \, d\theta + \frac{1}{2EA_1} \int_0^{2\pi} \frac{(P_1' + P_1'')^2}{r_1} \, d\theta + \frac{1}{2GA_1'} \int_0^{\pi} 2V_1^2 \, r_1 \, d\theta$$

$$= \tan^2\alpha \left\{0.00234 \left(\frac{r_1 \, M''^2}{EI_{r,1}}\right) + \frac{M^2}{2\pi EA_1 r_1} + 0.0744 \left(\frac{(1+\nu) \, M''^2}{EA_1' r_1}\right)\right\} \tag{33}$$

and there is a similar expression for the energy stored in the other ring. Thus, <u>for the case of stringers of constant section area</u> (in which M'' differs at each end of the frustum), we find

$$U_r = U_{r,1} + U_{r,2}$$

$$= \frac{M^2 \tan^2\alpha}{E}\left[0.00234 \, \mu^2 r_1 \left\{\frac{1}{(1+\mu)^2 \, I_{r,1}} + \frac{\beta}{(\beta+\mu)^2 \, I_{r,2}}\right\} + \frac{1}{2\pi r_1}\left(\frac{1}{A_1} + \frac{1}{\beta A_2}\right)\right.$$

$$\left. + \frac{0.0744 \, (1+\nu)\mu^2}{r_1}\left(\frac{1}{(1+\mu)^2 A_1'} + \frac{1}{\beta(\beta+\mu)^2 A_2'}\right)\right] \quad . \tag{34}$$

The total strain energy in the frustum is the sum of expressions (28) and (34). By equating this sum to expression (4) we can find, as before, the stiffness of an equivalent beam.

Dimensions of the reinforcing rings

At this point it is expedient to consider some typical dimensions of the reinforcing rings. To fix ideas, let us assume that the cross-section of the ring at s_1, say, is basically as shown in Fig.7. The dimensions w, h, t_r (the identification suffix 1 is omitted here) will now be determined by relating the maximum hoop stress in the ring to the maximum direct stress in the adjacent cylinder caused by the applied moment. Of course, in an actual structure the design requirements may be such that strict equality of these stresses is not appropriate, and for this reason we introduce an arbitrary proportionality constant γ, as in section 3.3.

For the section shown in Fig.7

$$\left.\begin{aligned} A_r &= t_r\,(h + 2w) \\ \text{and} \qquad I_r &= t_r h^2\,(h + 6w)/12 \;. \end{aligned}\right\} \tag{35}$$

The maximum hoop load P_{max} and the maximum moment m_{max} each occur at $\theta = 0, \pi$ and accordingly the maximum stress in the ring is given by

$$\begin{aligned} \sigma_{max} &= \frac{P_{max}}{A_r} + \frac{h m_{max}}{2I_r} \\ &= \frac{M \tan a}{\pi r_1 t_r\,(h + 2w)} + 0.447\,\frac{M'' \tan a}{h t_r\,(h + 6w)} \end{aligned} \tag{36}$$

in virtue of equations (29), (30), (32) and (35). If expression (36) is equated to $\gamma\sigma^*$, where σ^* is given by equation (18), we obtain the relation

$$\frac{h^2 t_r}{r_1^2 t} = \frac{\sin\alpha}{\gamma}\left\{\frac{1.40\mu}{1 + 6w/h} + \frac{h}{r_1}\left(\frac{1 + \mu}{1 + 2w/h}\right)\right\} . \tag{37}$$

To Investigate numerically the implications of this relation let us suppose that

$$\left.\begin{aligned} r_1/t &= 400 \;, \\ \mu &= 1 \;, \\ \alpha &= 10^\circ \;, \\ w &= \tfrac{1}{2}h \;, \\ \gamma &= 1.5 \;. \end{aligned}\right\} \tag{38}$$

An additional requirement, which follow8 from considerations of the stability of the ring, is that $h/t_r \leqslant 20$, say. If we tentatively assume that $h/t_r = 20$, equation8 (37) and (38) give

$$h = 0.142 \; r_1 \; .$$

In µiactice there will also be limitations on the magnitude of h, and if the preceding analysis yields an unacceptable value the ratio h/t, must be reduced. Thus in the present example, if the maximum allowable value of h is 0.1 r_1, say, equation (37) yield8

$$t_r = 0.13 \, h \quad . \tag{39}$$

There is a similar analysis for determining the dimensions of the ring at 8_2. Thus, corresponding to equation (37) we find, on introducing the identification suffix 2:

$$\frac{h_2^2 \, t_{r,2}}{r_2^2 \, t} = \frac{(1+\mu) \sin \alpha}{\gamma} \left\{ \frac{1.40 \mu}{(1 + 6w_2/h_2)(\mu + \beta)} - \frac{h_2/r_2}{1 + 2w_2/h_2} \right\} . \tag{40}$$

For the example specified by equation (38) with, let us say,

$$\left. \begin{aligned} \beta &= 1.45 \; , \\ h_2 &= 0.1 \; r_1 \; (=h) \end{aligned} \right\} \tag{41}$$

and

it is found from equation (40) that

$$t_{r,2} = 0.10 \; h \quad . \tag{42}$$

As for the strain energy stored in the rings, it follow8 from equation (34) that for a structure specified by equations (38), (39), (41) and (42),

$$u_r = 14.0 \frac{M^2}{Er_1^3} \; , \tag{43}$$

the contribution from the ring at s_2 being slightly greater than that at s_1. It is also of interest to note that the proportions of this energy due to bending, hoop loads and shear forces are approximately as 10:4:1. Finally we note that the strain energy U in the shell and stringers is given by expression (28), whence

$$U = 61.6 \frac{M^2}{Er_1^3} \quad . \tag{44}$$

A comparison of equations (43) and (44) shows that the stiffness of the conical frustum is about 20% less than that of a similar frustum with rigid ends.

3.5 The conical frustum shell with a separation capability

If the conical frustum shell has a separation capability the wall of the shell cannot be continuous across the separation line (or lines) and relatively heavy stringers must be provided to carry the axial and bending loads. There will also be a conflict of requirements in that the separation capability, involving the use of explosive bolts in the stringers, will be simpler if the number of stringers is small, whereas, for a given total stringer area, the overall flexural stiffness of the frustum will be greater if the stringers are more numerous. A detailed determination of the stresses is very difficult, but it is possible to make some general observations and to deduce some approximate results. First we note that because of the curvature of the shell the diffusion of load from the stringers into the adjacent shell wall will be markedly less than into a flat sheet; indeed, according to membrane theory there is <u>no</u> diffusion. Furthermore, even if some load diffusion does occur the diffusion process will be far from complete at the junctions with the adjacent cylinders, and this in turn means that the overall flexural stiffness of the cylinders is effectively reduced. If we assume, for purposes of estimating the overall flexural stiffness, that there is no diffusion in the frustum but complete diffusion in the cylinders the resulting errors are of opposite sign and therefore tend to cancel each other. Expressions for the overall stiffness for a structure with four continuous stringers may now be obtained by a limiting process from the results of section 3.4. Thus from equation (28) we find

$$U \approx \frac{M^2 \ell \, (r_1 + r_2)}{4\pi E \, r_1^2 \, r_2^2 \cos^3 \alpha} \left\{ \left(\frac{2\beta}{\beta+1}\right) \frac{1}{t_s} + \frac{2.47\,(1+\nu)\,\sin^2\alpha}{t} \right\} , \tag{45}$$

while from equation (34)

$$U_r \approx \frac{M^2 \tan^2\alpha}{E}\left\{0.00234\left(\frac{r_1}{I_{r,1}} + \frac{r_2}{I_{r,2}}\right) + \frac{1}{2\pi}\left(\frac{1}{r_1 A_1} + \frac{1}{r_2 A_2}\right) + 0.0744\,(1+\nu)\left(\frac{1}{r_1 A_1'} + \frac{1}{r_2 A_2'}\right)\right\} \quad . \qquad (46)$$

There is also a contribution from the reinforcing rings at separation lines:

$$\bar{U}_r \approx \frac{M^2 \tan^2\alpha}{E}\left\{0.000057 \sum \frac{r_n}{I_{r,n}} + 0.0430 \sum \frac{1}{r_n A_n} + 0.0045 \sum \frac{1+\nu}{r_n A_n'}\right\} \; . \qquad (47)$$

The derivation of equation (47) is given in Appendix C. It relates to the in-plane distortion of the rings and is based on the assumption that the only transfer of shear across a separation line occurs at the stringer positions ($\theta = 0, \pm\frac{1}{2}\pi, \pi$). It is also assumed that reinforcing rings adjacent to a common separation line have the same stiffness so that, from symmetry, a typical quadrant of a ring - bounded by $\theta = 0, \frac{1}{2}\pi$, say - is effectively clamped at $\theta = 0$ and simply supported at $\theta = \frac{1}{2}\pi$. The forces per unit length acting on such a ring are directed tangentially and are given by

$$T_\theta = N''_{s\theta} \, , \quad (M'' = M)$$

$$= \frac{M \tan a}{4 r_n} \quad . \qquad (48)$$

These forces cause the following hoop loads, shear forces and bending moments:

$$\left.\begin{aligned} P_n &= \frac{M \tan\alpha}{r_n}\,(0.208\cos\theta - 0.174\sin\theta) \quad , \\ V_n &= \frac{M \tan\alpha}{r_n}\,(0.250 - 0.174\cos\theta - 0.208\sin\theta) \quad , \\ m_n &= M\tan\alpha\,(0.219 - 0.250\,\theta - 0.208\cos\theta + 0.174\sin\theta) \quad . \end{aligned}\right\} \qquad (49)$$

<u>Optimum stringer area/skin thickness for maximum overall flexural stiffness</u>

The maximisation of the overall flexural stiffness is equivalent to minimisation of the expression ($U + U_r + \bar{U}_r$) defined by equations (45)-(47).

The terms t_s and t occur only in the expression for U (due, in part, to the underlying assumptions) and accordingly the optimum ratio t_s/t can be determined independently of the dimensions of the various reinforcing rings. Now the total weight of the skin and four stringers is proportional to

$$\left(\frac{\beta+1}{2}\right) t + t_s \quad . \tag{50}$$

If this total is kept constant, it may readily be shown that the minimum value of U occurs when

$$\mu = \frac{t_s}{t} = \frac{2A_s}{\pi r_1 t} = \left(\frac{\beta}{2.47\,(1+\nu)}\right)^{\frac{1}{2}} \operatorname{cosec} \alpha \, , \tag{51}$$

$$= 3.86 \text{ if } \beta = 1.45, \ \alpha = 10^\circ, \ \nu = 0.3 \text{ say} .$$

This expression must be regarded as an upper limit because of the underlying assumption of zero load diffusion from the stringers; if the skin is assumed to be 25% effective in carrying direct forces Ns, the optimum value for t_s/t is about 3.1 in the above example. [Equation (51) is appropriate to the frustum with four stringers. If the number of stringers is increased the assumption of zero load diffusion becomes increasingly untenable. The limiting case is when there is complete diffusion and the stringers can be regarded as a stringer-sheet. The optimum value of μ for this case can be obtained by minimisation of expression (9), subject to the constancy of expression (50). This results in the following equation for μ:

$$2(1+\nu)\,\mu^2 \sin^2\alpha + \frac{2\beta^2(\mu+\beta+1)}{\mu(\beta^2-1)} \ln\left(\frac{\beta(1+\mu)}{\beta+\mu}\right) = \beta + \frac{\beta^2(2\mu+\beta+1)}{(\beta+\mu)\,(\beta+1)\,(\mu+1)} \quad , \tag{52}$$

which yields a non-zero value of μ only when

$$6(1+\nu)\,\sin^2\alpha < (\beta-1)^2/\beta \quad .$$

'The fact that non-zero solutions are possible in certain circumstances is simply because the axial variation of the section area of the stringers (a constant) is nearer to the optimum variation, namely 1/s, than is that of the skin, which varies in direct proportion to s.]

Optimum thickness of reinforcing rings for maximum overall flexural stiffness

Let us now assume that the parameter μ is given - possibly by equation (51) - and that the reinforcing rings at the ends of the frustum are similar to that in Fig.7 with $w = \frac{1}{2}h$, so that - dropping the suffices 1,2 -

$$\left.\begin{aligned} A_r &= 2t_r h \ , \\ A'_r &= t_r h \ , \\ I_r &= \tfrac{1}{3} t_r h^3 \ . \end{aligned}\right\} \qquad (53)$$

If we further assume that h_1, h_2 are given, the corresponding optimum value of $t_{r,1}$ and $t_{r,2}$ may be determined in terms of t and the overall geometry of the frustum for maximum overall flexural stiffness. The total weight of the skin and stringers plus one (arbitrary) ring is proportional to

$$\frac{\pi \ell r_1 t}{\cos a}(1 + \beta + 2\mu) + 4\pi r h t_r \ .$$

If this total is kept constant while t and t_r are varied it may be shown that the overall flexural stiffness is a maximum when (with $\nu = 0.3$)

$$\frac{t_r}{t} = \frac{r_1 r_2 \sin a}{h^2}\left(\frac{\mu(1+\beta+2\mu)}{\beta + 1.60\mu\,(\beta+1)\sin^2 a}\right)^3 (0.011 + 0.276\ h^2/r^2)^{\frac{1}{2}} \ . \qquad \ldots (54)$$

If the reinforcing rings at separation lines are of the form specified by equation (53) it may likewise be shown that the overall flexural stiffness is a maximum when

$$\frac{t_r}{t} = \frac{r_1 r_2 \sin a}{h^2}\left(\frac{\mu(1+\beta+2\mu)}{\beta + 1.60\mu\,(\beta+1)\sin^2 a}\right)^{\frac{1}{2}} (0.00027 + 0.043\ h^2/r^2)^{\frac{1}{2}} \ . \qquad \ldots (55)$$

4 EXPERIMENTS ON XYLONl!l!E CONICAL FRUSTUM SHELLS

Tests on a series of models have been performed to gauge the efficacy of different methods for providing a (twin) separation capability without an undue drop in the overall flexural rigidity. For ease of manufacture the models, which have four equally spaced stringers, were constructed of xylonite (cellulose nitrate). There were basically two conical frustum shells with the same overall dimensions. In one of these the shell wall was continuous; the overall flexural stiffness of this model provided a yardstick against which the other(s) could be compared. The wall of the other shell was out along two circumferences; the overall flexural stiffness was then measured for this shell and for ten modified versions, the modifications including a variety of additional stiffening (and combinations thereof) including external reinforcing rings at the out edges, push-fit pins (axially orientated) connecting adjacent reinforcing rings, and an internal crossed shear bracing. The shells and the modifications are shown in Figs.8 and 9, while Fig.40 shows a model in the test rig. To simplify the interpretation of the results the ends of the shells were clamped to stiff attachments, as shown in Fig.9. The effect of flexible end attachments can, of course, be estimated from the preceding analysis.

4.1 Model dimensions

The dimensions of the uncut shell are

$$\ell = 10.5 \text{ in} ,$$

$$\alpha = 10^\circ ,$$

$$2r_1 = 8 \text{ in} ,$$

$$2r_2 = 11.7 \text{ in} ,$$

$$(\beta = r_2/r_1 = 1.46) ,$$

$$t = 0.040 \text{ in} ,$$

$$A_s = 0.3 \text{ in}^2 , \text{ (depth 0.6 in, width 0.5 in)} ,$$

$$\left(\mu = \frac{2A_s}{\pi r_1 t} = 1.19\right) ,$$

$$E = 280,000 \text{ lbf/in}^2 .$$

The structure extended an additional inch at each end to facilitate clamping to the stiff ply end fittings.

The shell with the twin separation capability is as specified above, but with circumferential cuts (0.075 in. wide) in the shell wall at axial distances from the smaller end of 2.7 in. and 6.6 in. The members of the internal crossed shear bracing are of square cross-section (0.3 in. × 0.3 in.) and each end is attached to a stringer by a 4 B.A. bolt, as shown in Fig.9. The four external reinforcing rings at the cut edges of the shell well are of two kinds, stiff and flexible. Each 'stiff' ring measures $\frac{1}{4}$ in. in the axial direction while the depth at the cut edge is 0.27 in.; the inner face of each ring is tapered to follow the skin surface to which it is glued: the outer face is cylindrical, so that the depth of the rings varies slightly in the axial direction. Holes of 3/32 in. diameter were drilled axially through adjacent rings at an angular spacing of 6°; a shear connection can thus be obtained by the insertion of 'push-fit' steel pins which bridge the gap across the cuts without detracting from the separation capability.

Each 'flexible' ring was obtained by cutting away sections of the 'stiff' ring between adjacent drill holes; this produced a castellated ring with adequate shear connection (with pins in) but negligible hoop and flexural rigidity. The rings were cut away to within 0.020 in. of the shell wall, and the width of each cut was such that the remaining sections were 0.0344 in. wide, i.e. (1/8 + 3/32 + 1/8) in. The flexible rings are shown on the frustum in Fig.8.

4.2 The tests

The tests were to determine the overall flexural stiffness of the models. A typical model, supported as a vertical cantilever, is shown in the test frame in Fig.10. The moment was applied to a horizontal steel channel beam bolted to the stiff upper end fitting. Did. gauge readings gave the rotation of this beam and hence the overall stiffness of the model. [A slight adjustment was made, by calibration, to account for bending of the beam itself.1 Separate tests were made with the stringers at $\theta = 0$, etc. end at $\theta = \frac{1}{4}\pi$, etc. although, in theory, the corresponding overall flexural stiffnesses should be the same. In practice the stiffness appropriate to the θ-zero position exceeded the other in all cases by about 10%. This feature can be attributed to differences in the efficiency of the end clamping of the skin and stringers. Here, only the average value of the two stiffnesses is quoted. Furthermore, for ease of interpretation, the overall flexural stiffnesses are expressed as fractions of the stiffness of the uncut shell. In this connection it is worth noting that the experimentally determined stiffness of the uncut shell agreed exactly with that derived from equations (4) and (28).

4.3 Test results

The overall flexural stiffness of the uncut frustum is, by definition, unity. In terms of this the stiffness of the cut frustum is 0.30. Table 1 shows the stiffness of the cut frustum with various reinforcements. The pin spacings quoted refer to the angular spacing between stringers so that, for example, a 45° spacing implies 4 pins per pair of adjacent rings; similarly 30° implies 8 pins.

Table 1

Relative stiffness of cut frustum with reinforcements

flexible rings, no pins	0.32
flexible rings, pins at 45°	0.49
flexible rings, pins at 30°	0.52
flexible rings, pins at $22\frac{1}{2}$	0.57
flexible rings, pins at 6°	0.74*
stiff rings, no pins	0.54
stiff rings, pins at 6°	0.74†
crossed bracing, no rings	0.52
crossed bracing, stiff rings, no pins	0.63
crossed bracing, stiff rings, pins at 6°	0.80

"Best buy.' Note the equality with line †. With continuous shear transfer there is no tendency for the rings to bend.

The test results demonstrate the importance of a multiple shear connection across a separation line. In an actual missile structure the rings would, of course, be on the inside and there would also be differences in the details of the shear connections.

5 CONCLUSIONS

Some aspects of the design of a conical frustum shell with a separation capability have been considered theoretically and experimentally. Particular attention has been paid to the determination of the overall flexural stiffness of the frustum, and to ways of maximising this stiffness. Such ways include the following:

(a) increasing the number of (continuous) stringers,

(b) optimum choice of stringer section area/skin section area,

(c) provision of multiple shear connections across a separation line,

(d) optimum design of reinforcing rings at the ends of the frustum (markedly dependent on (a)),

(e) ditto for rings at separation lines (markedly dependent on (c)),

(f) optimum tapering of skin and stringers (not discussed in detail).

Appendix A

STRESSES IN AN ANNULAR PLATE AT THE ENDS OF THE FRUSTUM

In this Appendix a stress-function solution is presented for the stresses in an annular plate of thickness t_r, bounded by inner and outer radii r_o, r_1 respectively; the loading on the outer boundary is given by equation (11) of the main text, while the inner boundary is free. The loads on the outer boundary cause radial and shear stresses

$$\left.\begin{aligned} (\sigma_r)_{r=r_1} &= K \cos\theta ,\\ (\tau_{r\theta})_{r=r_1} &= K \sin\theta ,\\ K &= \frac{Mtana}{\pi t_r r_1^2} \end{aligned}\right\} \qquad (56)$$

where

These stresses form a self-equilibrating system and, with the inner boundary being free of stress, equilibrium and compatibility throughout the annulus are satisfied by choosing a single-valued stress function which satisfies the biharmonic equation and the boundary conditions. A suitable function which satisfies the biharmonic equation is given by

$$\varphi = \tfrac{1}{2}(ar^3 + br^{-1}) \cos\theta , \qquad (57)$$

which yields stresses

$$\left.\begin{aligned} \sigma_r &= (ar - br^{-3}) \cos\theta ,\\ \sigma_\theta &= (3ar + br^{-3}) \cos\theta ,\\ \tau_{r\theta} &= (ar - br^{-3}) \sin\theta . \end{aligned}\right| \qquad (58)$$

The vanishing of the radial and shear stresses on the inner boundary is satisfied if

$$b = ar_o^4 ,$$

while the boundary conditions of equation (56) give

$$a\{r_1 - r_o^4/r_1^3\} = K .$$

Thus, introducing the notation

$$\left.\begin{aligned} \kappa &= r_o/r_1 \quad , \\ \rho &= r/r_1 \quad , \end{aligned}\right\} \tag{59}$$

yields

$$\left.\begin{aligned} \sigma_r &= \frac{K \cos\theta}{1-\kappa^4}\left(\rho - \kappa^4\rho^{-3}\right) \quad , \\ \sigma_\theta &= \frac{K \cos\theta}{1-\kappa^4}\left(3\rho + \kappa^4\rho^{-3}\right) \quad , \\ \tau_{r\theta} &= \frac{K \sin\theta}{1-\kappa^4}\left(\rho - \kappa^4\rho^{-3}\right) \quad . \end{aligned}\right\} \tag{60}$$

Now $\kappa \leq \rho \leq 1$ and, unless the annulus is deep, κ is only slightly less than unity. Accordingly the dominant stresses in the annulus are the hoop stresses σ_θ which vary (smoothly) between the values

$$(\sigma_\theta)_{r=r_0} = -\left(\frac{4\kappa}{1-\kappa^4}\right) \cos\theta$$

and

$$(\sigma_\theta)_{r=r_1} = \left(\frac{3+\kappa^4}{1-\kappa^4}\right) K \cos\theta \quad .$$

Further, as $\kappa \to 1$ the hoop stresses remain virtually constant across the width of the annulus and the hoop load is given by

$$\begin{aligned} P_1 &= \int_{r_0}^{r_1} t_r \sigma_\theta \, dr \quad , \\ &= K t_r r_1 \cos\theta \quad , \\ &= \left(\frac{M \tan\alpha}{\pi r_1}\right) \cos\theta \quad , \end{aligned} \tag{12 bis}$$

in virtue of equation (56).

Appendix B

THE LOADS IN THE REINFORCING RINGS AT THE ENDS OF THE FRUSTUM

In this Appendix we determine the loads in a reinforcing ring due to the double-dashed system discussed on page 13. Account is taken of the direct, shear and flexural stiffness of the ring, and of the eccentricity of the applied loads T_θ. It is shown, however, that the more usual analysis which takes account only of the flexural stiffness of the ring is sufficiently accurate; attention is confined to this simpler analysis in Appendix C.

The loads applied to the half ring bounded by $0 \; 6 \; \theta \; 6 \; \pi$ are shown diagrammatically in Fig.11 where, for convenience, the end forces and moments are expressed in terms of fictitious values at the origin. The loads in the other half of the ring are, of course, a mirror image of these and it follows that there are no resultant vertical 'opening forces' at the origin. The vertical (downward) forces V_o applied at $\theta = 0, \pi$ are equal to $\frac{1}{2}P_s$ sin a, which is also the shear force in the ring at $\theta = 0$; hence the notation V_o. In addition, the total anti-clockwise bending moment at the origin is equal to $\pi V_o r$ and this is shown, for convenience, as applied in equal proportions to the two fictitious arms. There remain two self-equilibrating systems at the origin, namely equal and opposite horizontal forces P_o and moments m'; these are to be determined by the boundary conditions. The following additional notation is introduced,

$$\bar{r} = \text{radius to centroid of ring},$$

$$\lambda = (r-\bar{r})/\bar{r} \quad ,$$

$$k = \frac{EI_r}{\bar{r}^2 G A'} \quad .$$

The moment in the ring $m(\theta)$ is the sum of the following components:

$$\left.\begin{aligned}
[m]_{\text{moment at origin}} &= m' + \frac{\pi}{2} V_o r \ , \\
[m]_{\text{vertical shear at origin}} &= - V_o \bar{r} \sin\theta \ , \\
[m]_{\text{horizontal force at origin}} &= P_o \bar{r} \cos\theta \ , \\
[m]_{\text{shear flow } T_\theta \text{ at centroid}} &= - V_o \bar{r} \int_0^\theta (1 - \cos\varphi)\, d\varphi \\
&= - V_o \bar{r} (\theta - \sin\theta) \ , \\
[m]_{\text{eccentricity of shear flow } T_\theta} &= - V_o (r - \bar{r}) \theta \ ,
\end{aligned}\right| \qquad (61)$$

whence, on addition,

$$m(\theta) = m' + \frac{\pi}{2} V_o r - V_o r\theta + P_o \bar{r} \cos\theta \ . \qquad (62)$$

Similarly the shear force in the ring is given by

$$V = V_o + P_o \sin\theta \ , \qquad (63)$$

and the hoop load is given by

$$P = P_o \cos\theta \ . \qquad (64)$$

The boundary conditions are such that if the ring is regarded as clamped at $\theta = 0$, the slope due to bending and the horizontal displacement are zero at $\theta = \pi$. The vanishing of the slope due to bending implies that

$$\int_0^\pi m(\theta)\, d\theta = 0 \ ,$$

so that

$$m' = 0 \ . \qquad (65)$$

The component of the horizontal displacement at $\theta = \pi$ due to bending is given by

$$\frac{\bar{r}^2}{EI_r}\int_0^\pi m(\theta)\,(1+\cos\theta)\,d\theta \quad ,$$

and that due to shear is given by

$$\frac{\bar{r}}{GA'}\int_0^\pi v\sin\theta\,d\theta \quad ,$$

while that due to the hoop load vanishes identically. Equating to zero the sum of these expressions yields

$$P_0 = -\frac{4}{\pi}V_o\left(1+\frac{\lambda}{1+k}\right) \quad . \tag{66}$$

The parameter λ is small in comparison with unity so that we may write

$$P_o \approx -\frac{4}{\pi}V_o$$

which is the value obtained from elementary theory which takes account only of the flexural stiffness of the ring. In terms of V_o we now find

$$\left.\begin{aligned} m(\theta) &\approx V_o r\left(\frac{\pi}{2}-\theta-\frac{4}{\pi}\cos\theta\right) , \\ v &\approx V_\theta\left(1-\frac{4}{\pi}\sin\theta\right) , \\ P &\approx -\frac{4}{\pi}V_o\cos\theta \ . \end{aligned}\right\} \tag{67}$$

Equations (30)-(32) of the main text are recovered by writing

$$V_0 = \tfrac{1}{2}P_s\sin a = \frac{M''}{4s\cos\alpha}$$

in virtue of equation (22).

Appendix C

THE LOADS IN THE REINFORCING RINGS AT SEPARATION LINES

This Appendix gives the derivation of equation (49), and hence equation (47), of the main text. The analysis does not take account of the direct end shear stiffness of the ring or the eccentricity of the applied loads T_θ. The loads acting on a quadrant of ring bounded by $0 \leqslant \theta \leqslant \frac{1}{2}\pi$ are shown in Fig.12, where the tangential force per unit length T_θ is denoted by F/r and is given by equation (48). Vertical and horizontal equilibrium of these tangential forces is provided by the forces F shown at the point B. The forces V_o, P_o and moment m_o are to be determined from overall moment equilibrium and from the boundary conditions.

The moment $m(\theta)$ is given by

$$m(\theta) = m_o - V_o r \sin\theta - P_o r(1-\cos\theta) - Fr(\theta - \sin\theta) \quad . \tag{68}$$

The vanishing of $m(\frac{1}{2}\pi)$ leads to the relation

$$m_o = r\{V_o + P_o + F(\tfrac{1}{2}\pi - 1)\} \tag{69}$$

and hence, in terms of V_o, P_o,

$$m(\theta)/r = P_o \cos\theta + (V_o - F)(1 - \sin\theta) + F(\tfrac{1}{2}\pi - \theta) \ . \tag{70}$$

The boundary conditions of simple support at B and clamping at A can be expressed by equating to zero the horizontal and vertical displacements at B, assuming no displacement or rotation at A. The displacements at B are readily given by integrating the curvature changes multiplied by the appropriate perpendicular arms. Thus

$$\int_0^{\frac{1}{2}\pi} m(\theta) \cos\theta \, d\theta = 0 \ ,$$

and (71)

$$\int_0^{\frac{1}{2}\pi} m(\theta)(1 - \sin\theta) \, d\theta = 0 \ .$$

Substitution of equation (70) into equations (71) and solving for V_o, P_o gives

$$\left.\begin{aligned} \frac{V_o}{F} &= \frac{8 - 24\pi + 10\pi^2 - \pi^3}{6\pi^2 - 16\pi - 8} \quad , \\ \text{and} \qquad & \\ \frac{P_o}{F} &= \frac{40 - 16\pi + \pi^2}{3\pi^2 - 8\pi - 4} \quad . \end{aligned}\right\} \tag{72}$$

Expressions (70) and (72) suffice to determine the bending moment $m(\theta)$, while the shear force and hoop load may be determined from the relations:

$$\begin{aligned} V &= V_o \cos\theta + P_o \sin\theta + F(1 - \cos\theta) \ , \\ P &= P_o \cos\theta + (F - V_o) \sin\theta \end{aligned} \tag{73}$$

REFERENCES

NO.	Author	Title. etc.
1	W. Flügge	"Stresses in Shells", Springer-Verlag, 1960

The following papers are on topics closely related to the present investigation:

2	A. Walöen	Asymmetrical loading of conical shells. Trans. Roy. Inst. Technol., Stockholm No.218, 1963
3	H. Becker	Design of cylinder-cone intersections. J. Spacecraft and Rockets **1**, 1, 120-122, Jan/Feb 1964
4	B. Wilson	Asymmetrical bending of conical shells. Proc. Amer. Soc. Civ. Engrs. 86, EN3, 119-139, June 1960

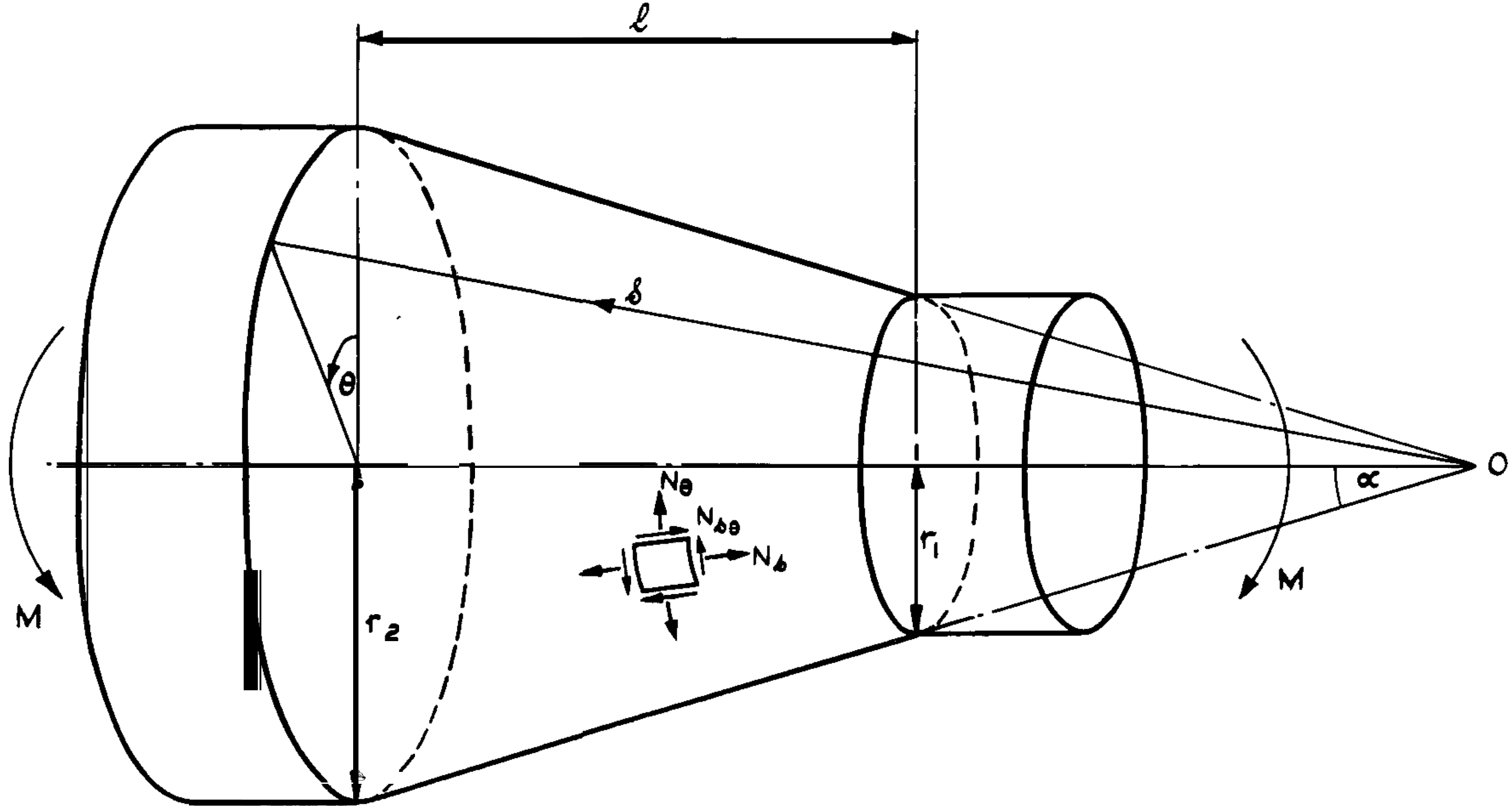

Fig. 1 The conical frustum shell.

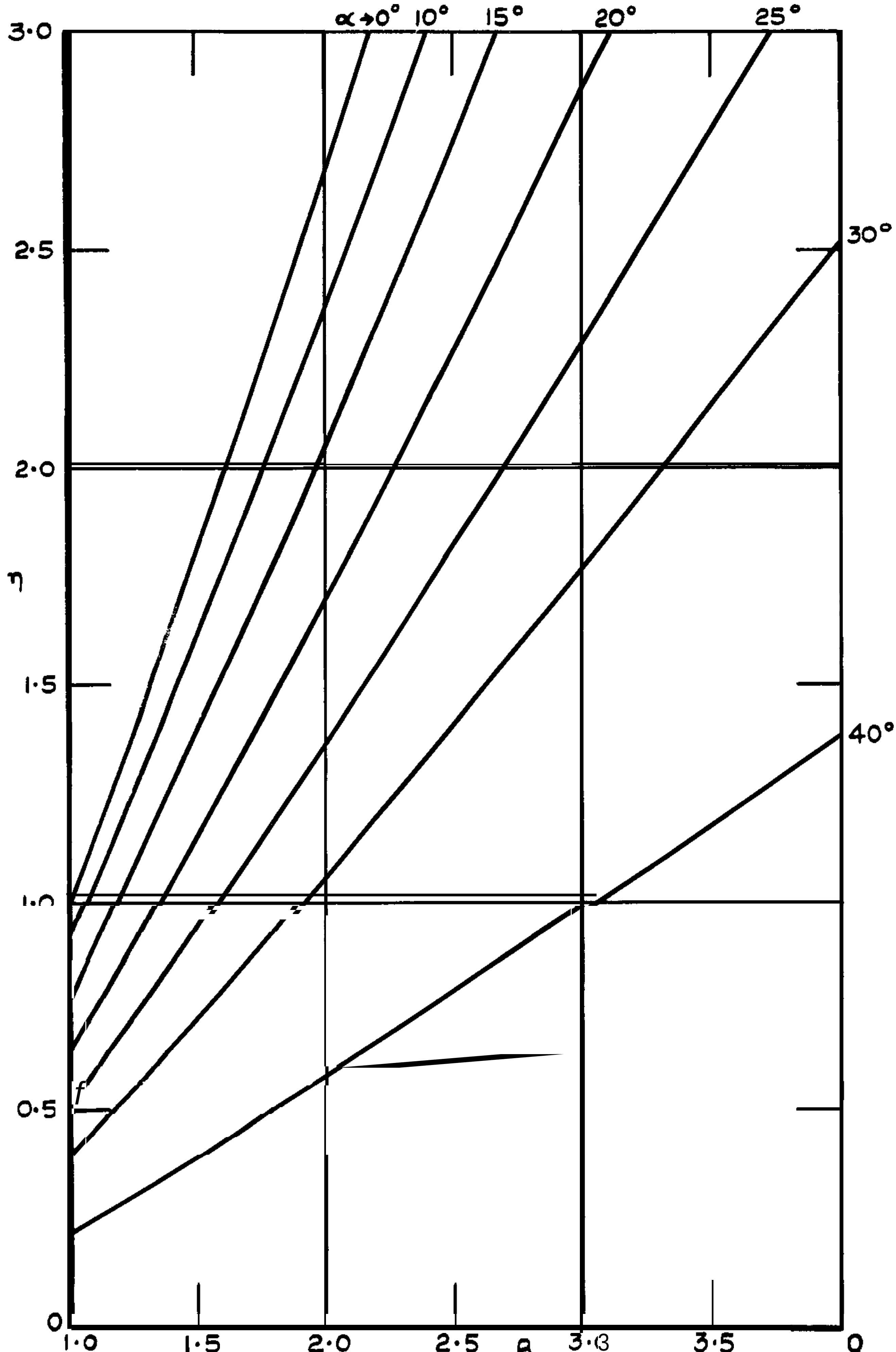

Fig. 2 Flexural stiffness of unreinforced frustum shell, rigid ends.

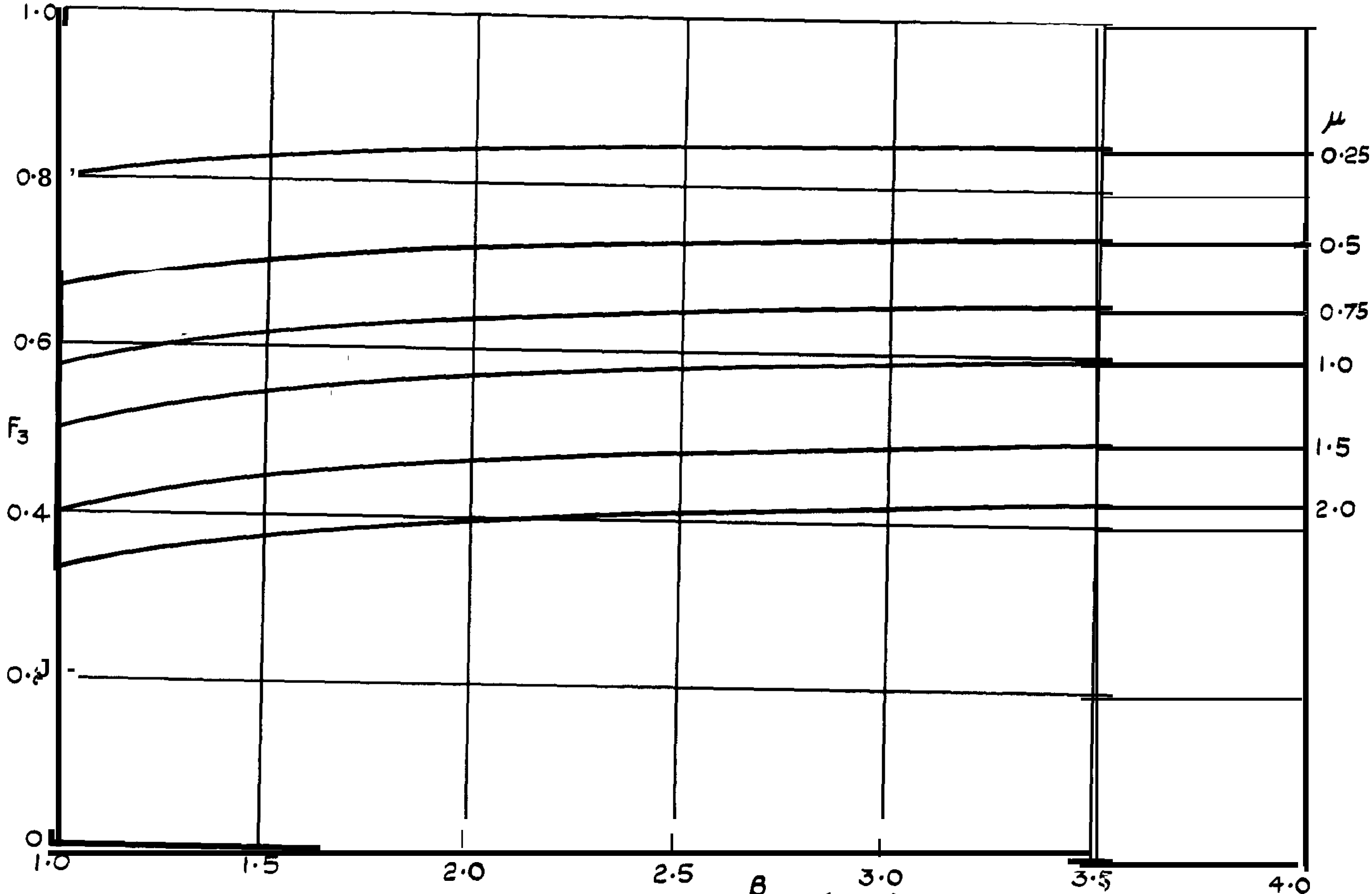

Fig. 3 The function $F_3(\beta, \mu)$

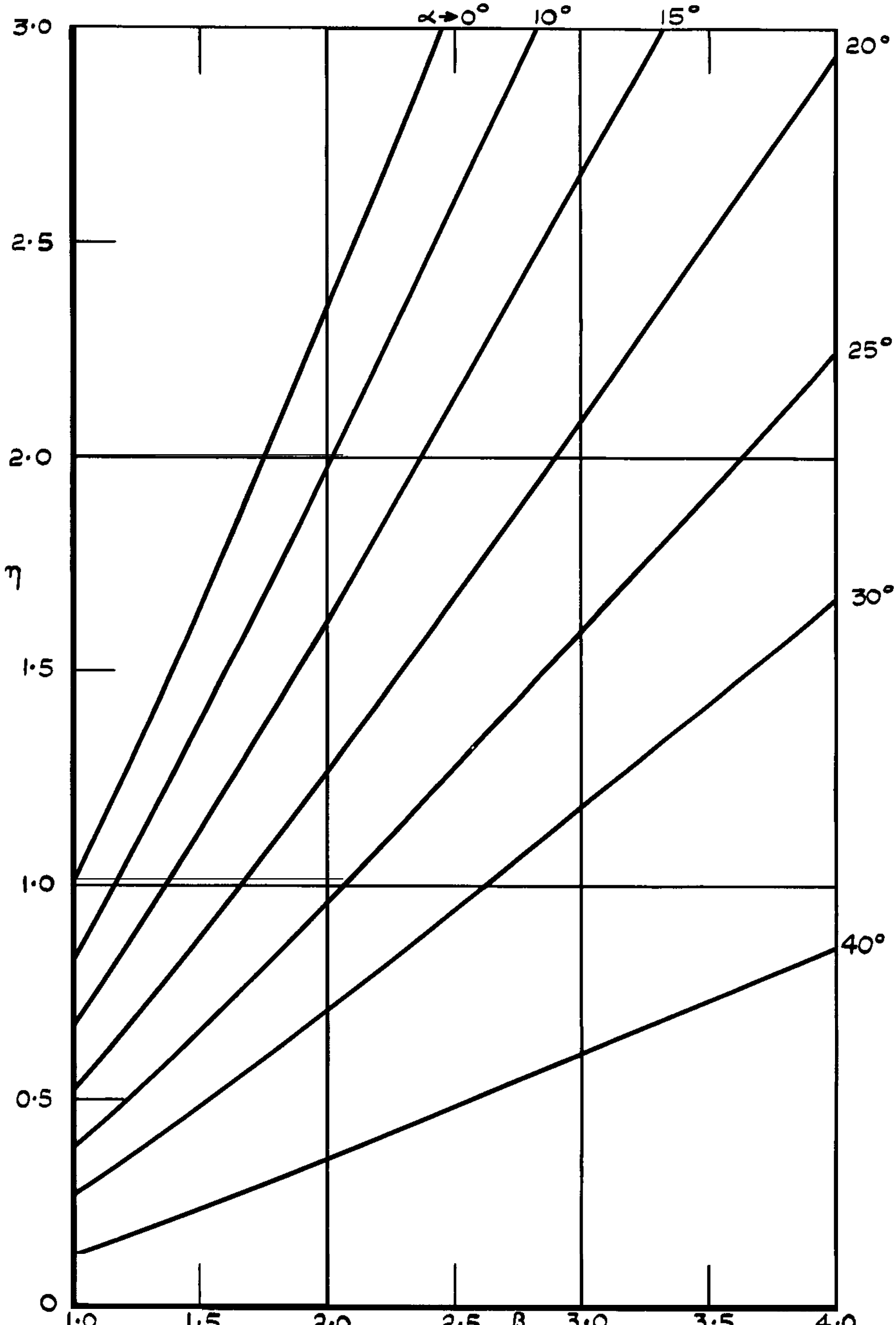

Fig. 4 Flexural stiffnes s of reinforced frustum shell, rigid ends($\mu = 1$)

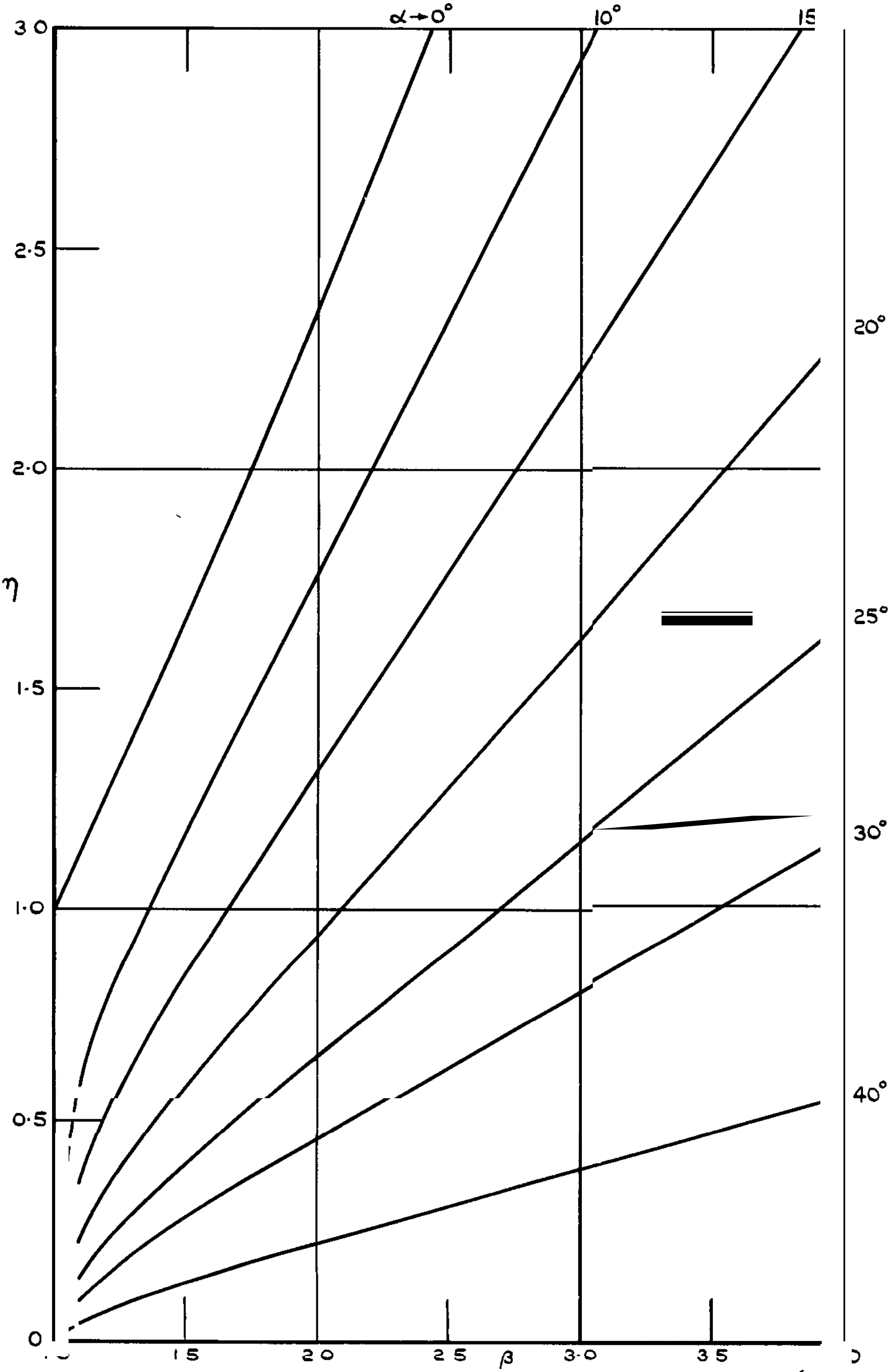

Fig.5 **Flexural** stiffness of reinforced frustum shell, flexible ends (μ=1, γ=1)

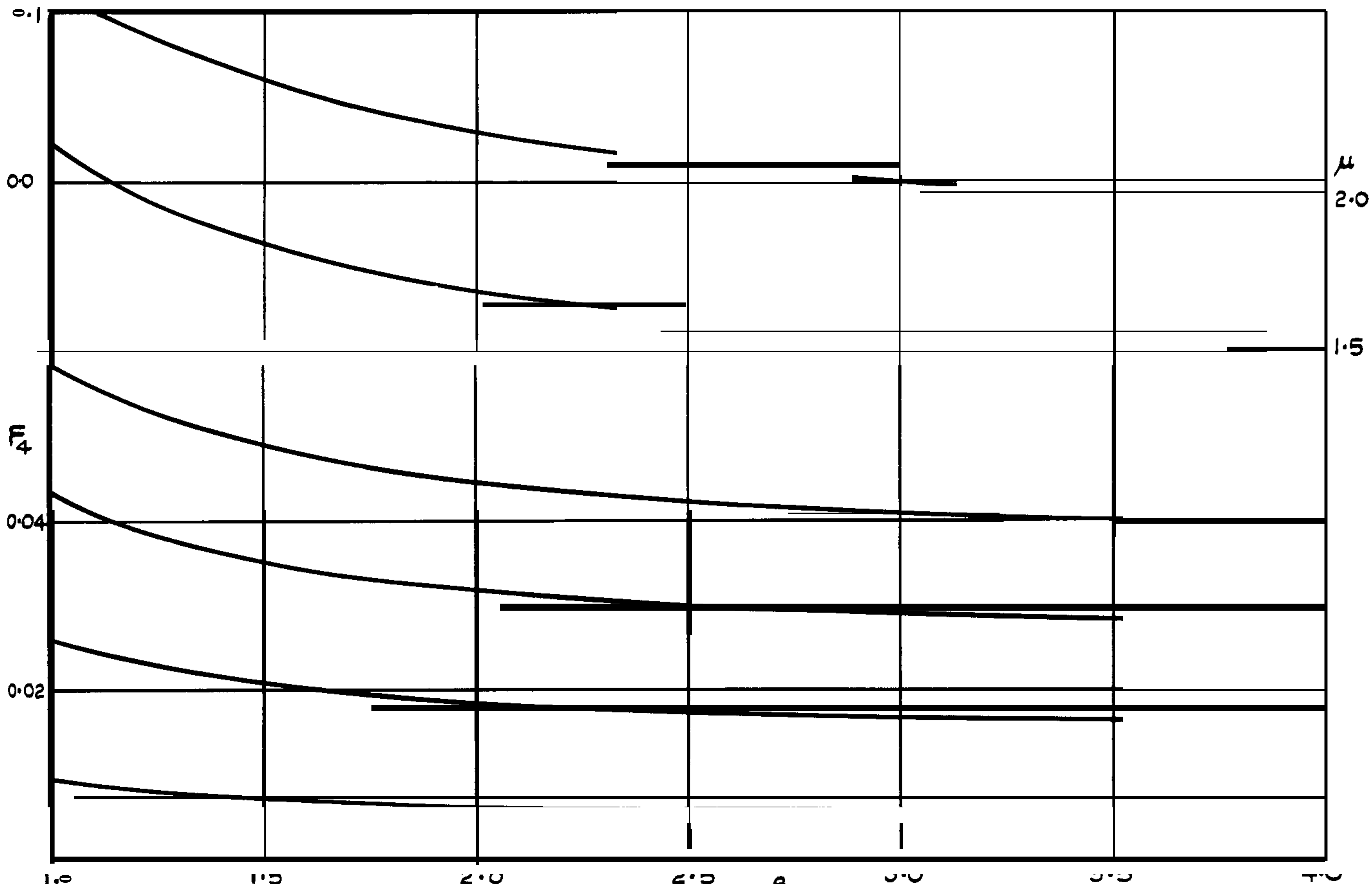

Fig. 6 The function $F_4(\beta, \mu)$

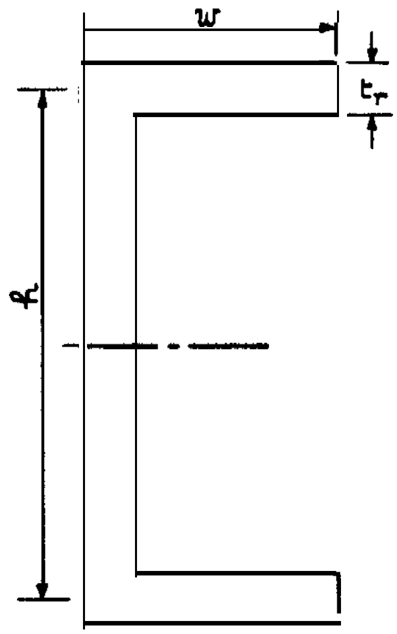

Fig.7 Cross-section of reinforcing ring

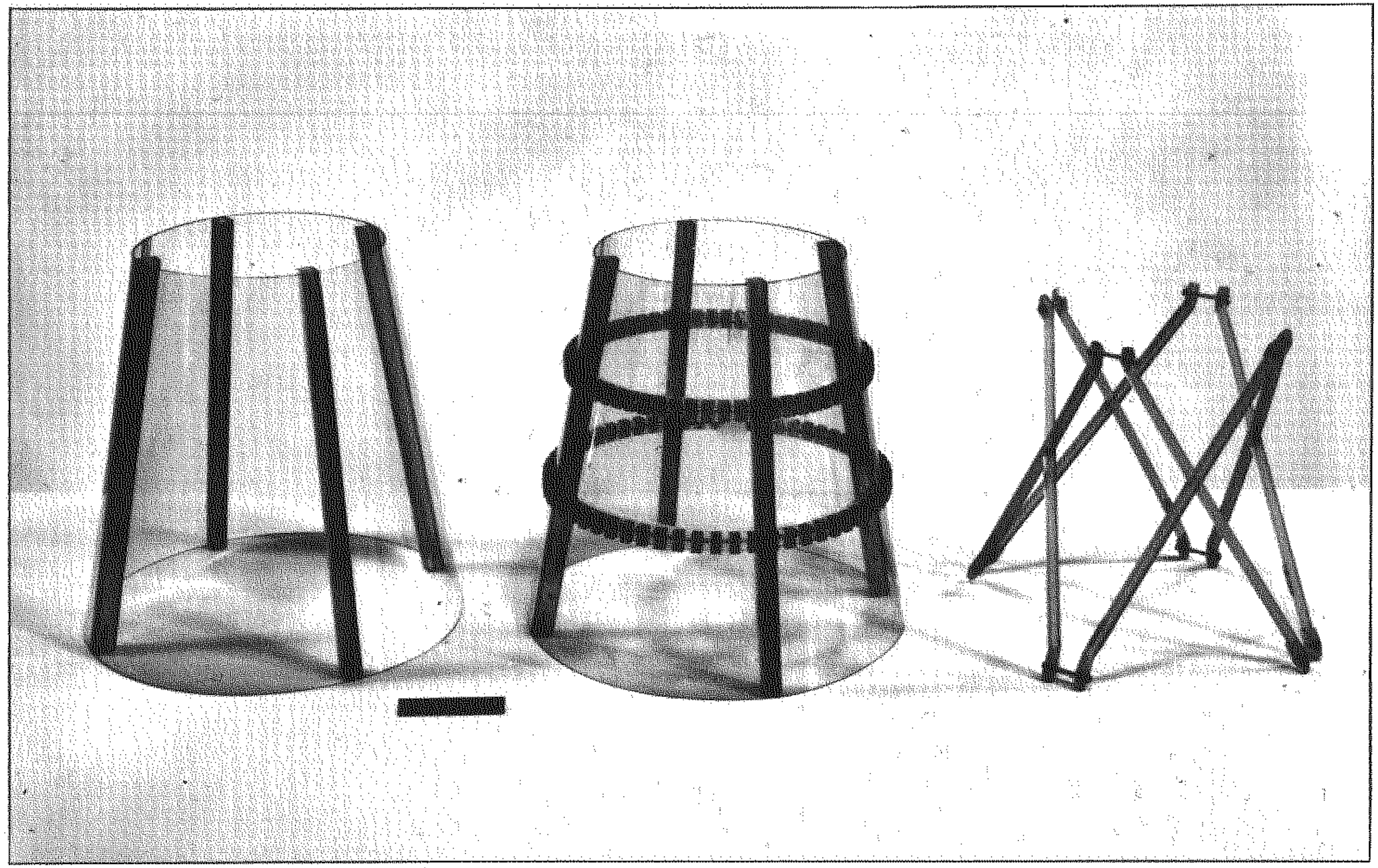

Fig.8 The uncut frustum, the cut frustum with flexible rings, and the crossed shear bracing

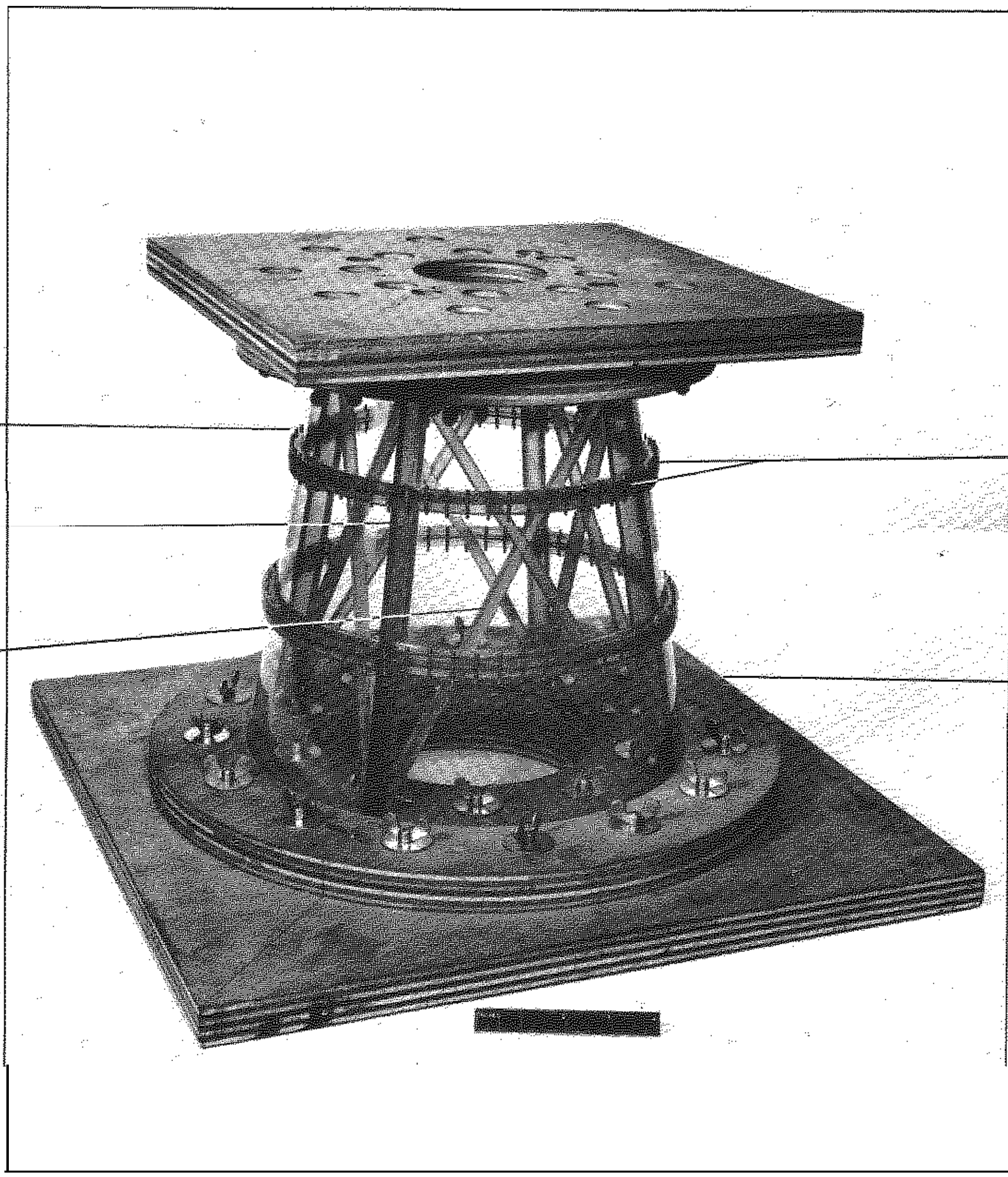

Fig.9 Xylonite model with twin separation capability

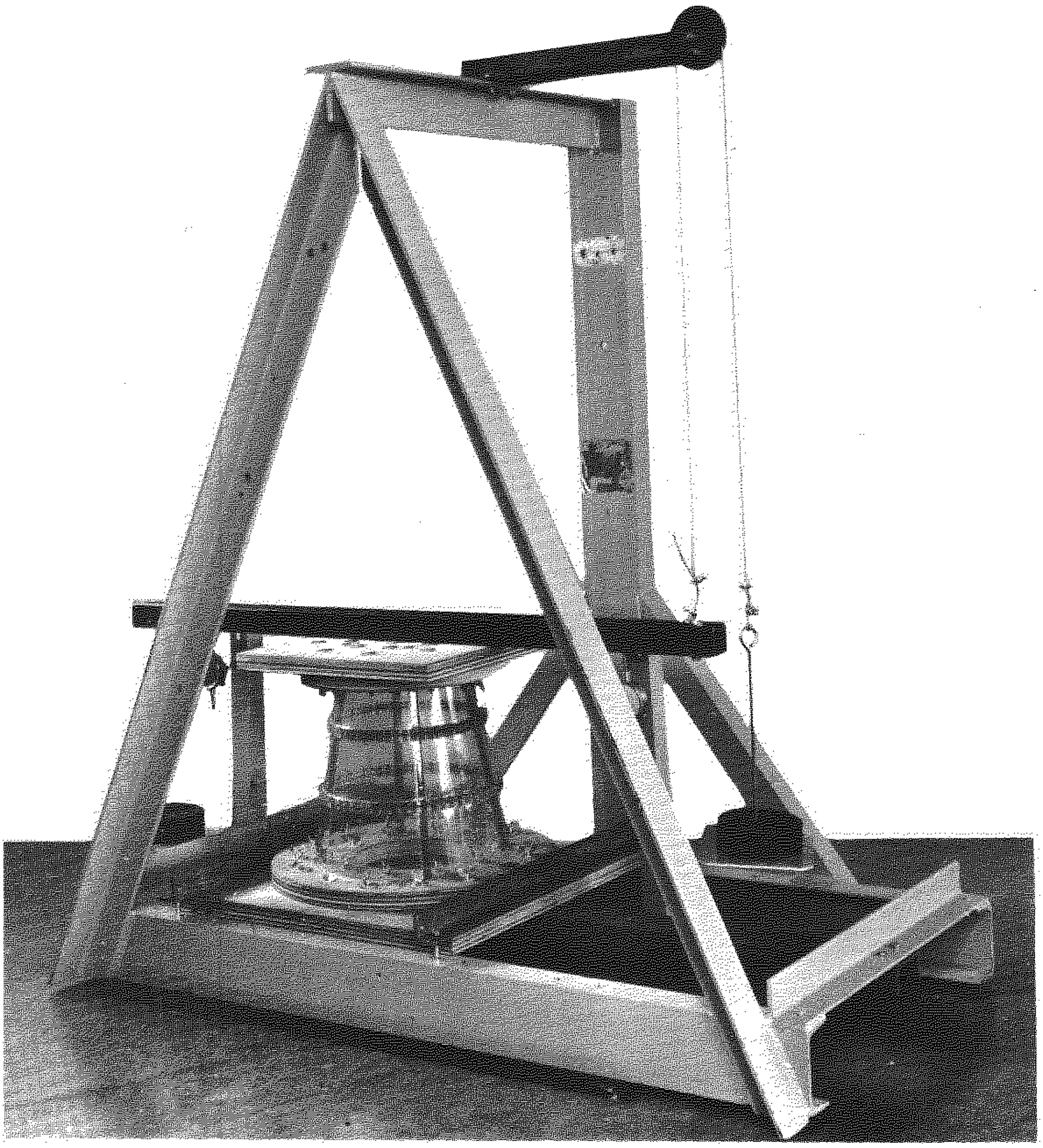

Fig.10 A model in the test rig

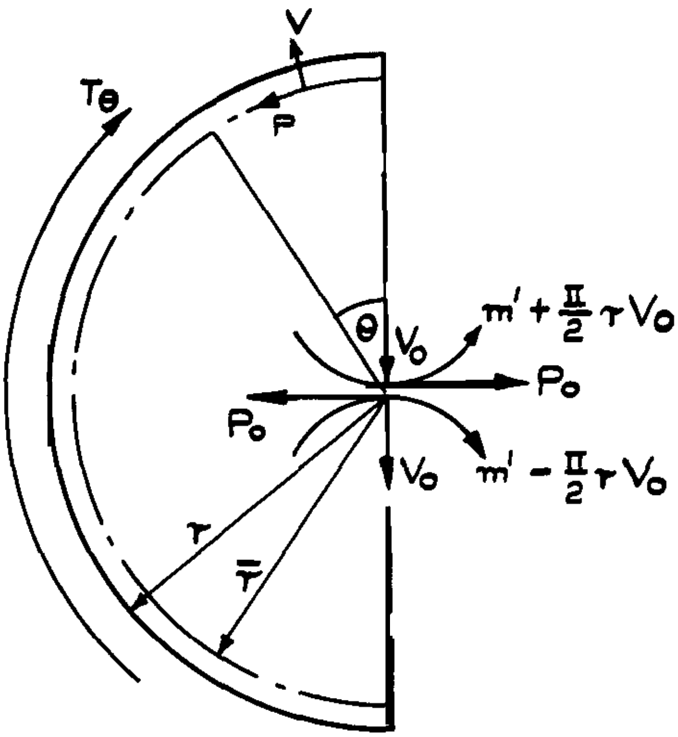

Fig. 11 Loads acting on half ring at end of frustum.

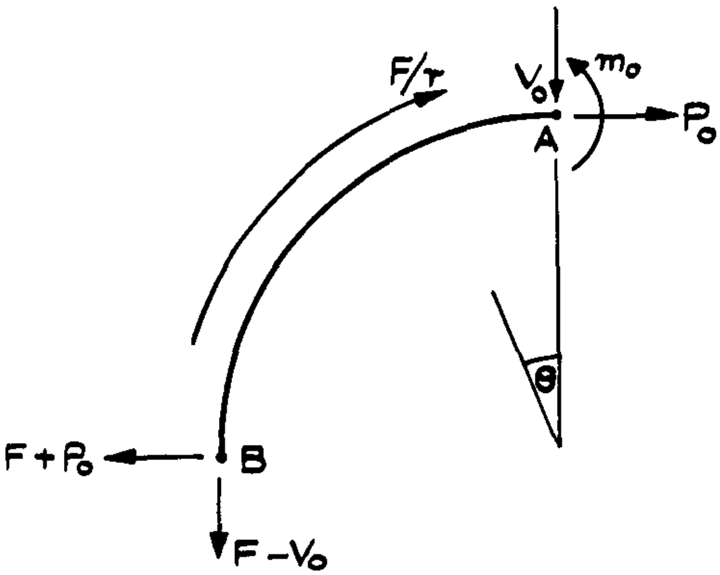

Fig. 12 Loads acting on quadrant of ring at separation line.

Printed in England for Her Majesty's Stationery Office by
the Royal Aircraft Establishment, Farnborough. Dd.135845. X.3

A.R.C. C.P. No.1039
October 1967

Mansfield, E.H.

ON THE FLEXURE OF A CONICAL FRUSTUM SHELL

539.384 :
621-434.1 :
621-434.5 :
621-448.1 :
624.078.8 :
621.887 :
629.19.012.25

This Report considers theoretically and experimentally some of the problems associated with the flexure of two unequal cylindrical shells joined by a conical frustum. Particular attention is given to the determination of the overall flexural stiffness of the conical frustum and to structural design considerations associated with the provision of a separation capability in the frustum. The results are particularly relevant to the design of multi-stage rockets.

A.R.C. C.P. No.1039
October 1967

Mansfield, E.H.

ON THE FLEXURE OF A CONICAL FRUSTUM SHELL

539.384 :
621-434.1 :
621-434.5 :
621-448.1 :
624.078.8 :
621.887 :
629.19.012.25

This Report considers theoretically and experimentally some of the problems associated with the flexure of two unequal cylindrical shells joined by a conical frustum. Particular attention is given to the determination of the overall flexural stiffness of the conical frustum and to structural design considerations associated with the provision of a separation capability in the frustum. The results are particularly relevant to the design of multi-stage rockets.

A.R.C. C.P. No.1039
October 1967

Mansfield, E.H.

ON THE FLEXURE OF A CONICAL FRUSTUM SHELL

539.384 :
621-434.1 :
621-434.5 :
621-448.1 :
624.078.8 :
621.887 :
629.19.012.25

This Report considers theoretically and experimentally some of the problems associated with the flexure of two unequal cylindrical shells joined by a conical frustum. Particular attention is given to the determination of the overall flexural stiffness of the conical frustum and to structural design considerations associated with the provision of a separation capability in the frustum. The results are particularly relevant to the design of multi-stage rockets.

DETACHABLE ABSTRACT CARDS

C.P. No. 1039

Published by
HER MAJESTY'S STATIONERY OFFICE

To be purchased from
49 High Holborn, London W C 1
13A Castle Street, Edinburgh 2
109 St Mary Street, Cardiff CF1 1JW
Brazennose Street, Manchester 2
50 Fairfax Street, Bristol BS1 3DE
258 Broad Street, Birmingham 1
1 Linenhall Street, Belfast BT2 8AY
or through any bookseller

C.P. No. 1039

SBN 11 470166 0